Modeling and Characterization of the Bonding-Wire Interconnection

Federico Alimenti, *Associate Member, IEEE*, Paolo Mezzanotte, Luca Roselli, *Member, IEEE*, and Roberto Sorrentino, *Fellow, IEEE*

***Abstract*—In this paper, the bonding-wire interconnection has been studied from the points of view of its modeling and electrical characterization. Both single- and double-wire structures have been considered, the latter under the assumption of parallel wires. Two electrical models of the bonding wire are discussed. First, the finite-difference time-domain (FDTD) method is proposed for the rigorous analysis of such structures. This method uses a suitable discretization technique, which accounts for the wire curvature by means of a polygonal approximation. A quasi-static model of the bonding wire, suitable for commercial microwave computer-aided-design tools is then proposed. This model is based on the representation of the structure with four sections of a uniform transmission line and the model parameters are evaluated analytically from the dimensions of the interconnection. Accuracy and applicability of the quasi-static model have been assessed by analyzing several test structures, the reference results being obtained with the FDTD method. Finally, the quasi-static model has been used to provide an extensive electrical characterization of the bonding wire versus its main geometrical parameters. This characterization is given in terms of an equivalent series inductance and two equivalent shunt capacitances forming a π low-pass network. This representation is particularly useful in the matching of the bonding-wire discontinuity.**

***Index Terms*—Bonding wire, CAD, FDTD, interconnections, packaging.**

I. Introduction

THE bonding wire is a very popular interconnection technology adopted in the fabrication of both microwave integrated circuits (MICs) and monolithic microwave integrated circuits (MMICs). It is employed to connect solid-state devices to passive circuit elements, as well as multichip modules. In spite of its small physical length, when millimeter-wave operations are required, the discontinuity introduced by the bonding wire can significantly affect the performance of the whole circuit [1]–[4].

To alleviate this problem, flip-chip [5]–[7] and electromagnetic coupling interconnects [8], [9] have been proposed. Nonetheless, the bonding wire, well established in consumer electronics, remains a very attractive solution since it is robust and inexpensive. In addition, it has the advantage of being tolerant of chip thermal expansion (or contraction); an important requirement in many applications, particularly for space-qualified systems.

Manuscript received July 29, 1999. This work was supported in part by the Italian Spatial Agency under Contract 1/R/092/00.

The authors are with the Department of Electronic and Information Engineering, University of Perugia, I-06125 Perugia, Italy (e-mail: alimenti@diei.unipg.it).

Publisher Item Identifier S 0018-9480(01)00016-3.

Accurate models of the bonding-wire interconnect are, therefore, necessary for an effective design of MMICs operating in the millimeter-wave range. Two models are presented in this paper with different degrees of accuracy. A rigorous electromagnetic model based on the finite-difference time-domain (FDTD) method is presented first. The model uses an appropriate discretization technique to obtain a polygonal approximation of the wire curvature. A quasi-static model is then proposed, the interconnection being represented as the cascade of four uniform transmission-line sections. Such a model is suitable for commercial microwave computer-aided design (CAD) tools since its parameters can simply be evaluated analytically from the dimensions of the structure. The FDTD and quasi-static models are applied to both single- and double-wire interconnections. In the latter case, the wires are assumed to be parallel.

To validate the analysis methods developed, the FDTD model was first compared with experimental data available in the literature showing a very good agreement. The FDTD model was then used as a reference in order to assess the accuracy and applicability of the quasi-static model.

Finally, an extensive analysis was carried out using the quasi-static model in order to characterize the electrical performances of single- and double-wire interconnections in terms of wire length and height. The characterization is given in terms of an equivalent low-pass π-network. Such representation is very useful in the design of networks capable of compensating for the bonding-wire discontinuity. In particular, the capability of adjusting the wire spacing and, thus, the equivalent inductance of double-wire structures, is an additional degree of freedom that can be used to reduce the sensitivity of the interconnection to the mechanical tolerances in the chip positioning.

II. Modeling

In this section, two electrical models of the bonding-wire interconnection are discussed. First, a full-wave model based on the FDTD method is introduced. This model is used to rigorously analyze several bonding-wire configurations (including multichip, single-, and double-wire structures) and to produce reference results. A quasi-static model is then described. It is derived by approximating the interconnection with four uniform transmission-line sections. Such a model is suitable for commercial microwave CAD tools since its parameters can be evaluated analytically from the dimensions of the structure. These dimensions define a geometrical model, which is described in the following.

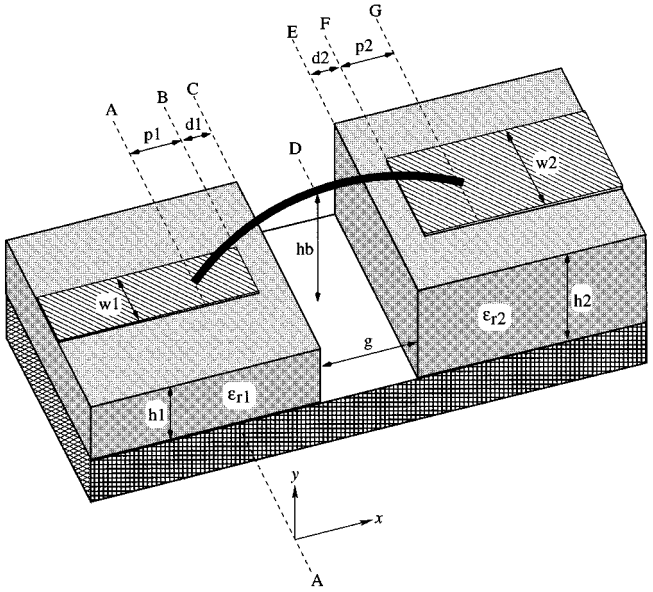

(a)

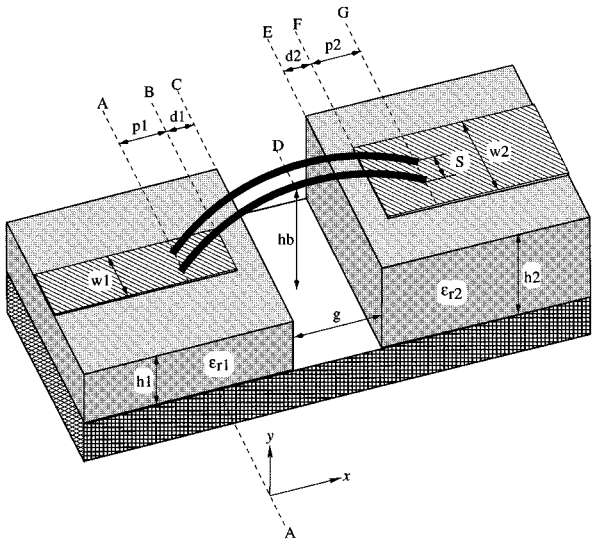

(b)

Fig. 1. Geometry of the bonding wire. (a) Single-wire interconnection. (b) Double-wire interconnection.

A. Geometrical Model

The geometries of single- and double-wire interconnections are depicted in Fig. 1(a) and (b), respectively. In the latter case, the wires are assumed to be parallel. The distance between the soldering points of each wire is given by

$$d_b = p_1 + d_1 + g + d_2 + p_2. \tag{1}$$

The curvature of the bonding wire has been approximated as an arc of a circle. With reference to the coordinate systems of Fig. 1, the height of each wire from the ground plane can thus be expressed as

$$h(x) = y_c + \sqrt{r_c^2 - (x - x_c)^2} \tag{2}$$

where r_c and x_c, y_c are the radius, and the x- and y-coordinates of the center. These parameters are determined as in Table I by

TABLE I
CIRCLE PARAMETERS. $\Delta = b^2 - 4ac$

$a = 1 - \dfrac{h_b - h_2}{h_b - h_1}$	$b = -2\,d_b$	$c = d_b^2 + (h_1 - h_2)(h_b - h_2)$
$x_c = \begin{cases} \frac{d_b}{2}, & a = 0 \\ -\frac{b+\sqrt{\Delta}}{2a}, & \Delta \geq 0 \end{cases}$	$y_c = \dfrac{h_b^2 - h_1^2 - x_c^2}{2(h_b - h_1)}$	$r_c = h_b - y_c$

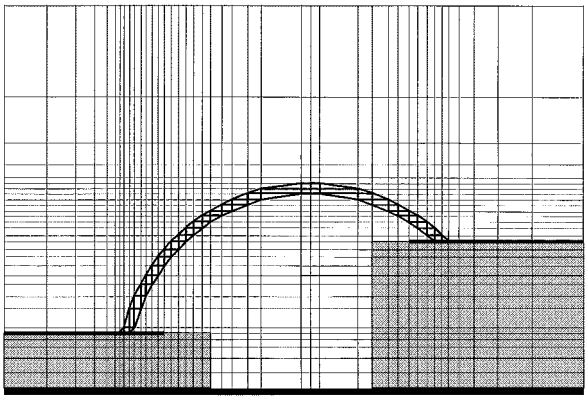

Fig. 2. Nonuniform mesh and polygonal approximation of the bonding wire.

the specific dimensions of the structure d_b, h_1, h_2 and h_b, shown in Fig. 1. The dimension h_b is the distance between the highest point of the bonding wire and ground plane.

B. FDTD Model

The discretization technique proposed in [10] and [11] was adopted for the FDTD analysis of the structures of Fig. 1. This technique can be explained as follows. First, a graded mesh [12] capable of fitting the boundaries of the bonding wire is constructed. Grid nodes are located on the wire contour using the staircases of Fig. 2. Observe that in order to identify each staircase, it is sufficient to establish the position of one step. This position is a degree of freedom that allows additional constraints to be satisfied. For example, the ends of the microstrips (lines B and F in Fig. 1) and the substrate boundaries (lines C and E in Fig. 1). In the case of Fig. 2, two staircases are needed to satisfy such constraints. Additional staircases may be used to refine the discretization.

A polygonal approximation of the curved metal contour can then be achieved by adopting triangular cell field updating, as described in [13]. The cross section of the wire is approximated as a square. Outside the wire region, the technique proposed in [14] has been adopted for an optimum mesh grading.

The perfectly matched layer (PML) boundary condition [15] and the excitation technique proposed in [16] was adopted to evaluate the scattering parameters of the bonding wire. Two uniform microstrip lines were used to feed the structure. The lengths of these lines were chosen in such a way that higher order modes at the reference planes have negligible amplitude. The incident wave was obtained by presimulating a uniform microstrip line.

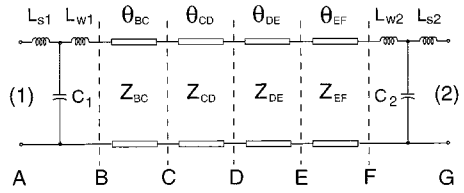

Fig. 3. Quasi-static model.

TABLE II
LINE PARAMETERS. $Z_c(x)$ IS THE LOCAL IMPEDANCE COMPUTED WITH (4) FOR SINGLE WIRE AND WITH (12) FOR DOUBLE WIRE. Z AND θ ARE THE CHARACTERISTIC IMPEDANCE AND ELECTRICAL LENGTH OF EACH SECTION IN FIG. 3. $\beta_0 = \omega\sqrt{\mu_0\epsilon_0}$

section	x_p	Z	θ
BC	$p_1 + \frac{d_1}{2}$	$Z_c(x_p)$	$\beta_0\, d_1\, [\epsilon_w(x_p)]^{\frac{1}{2}}$
CD	$\frac{x_c + p_1 + d_1}{2}$	$Z_c(x_p)$	$\beta_0\ (x_c - p_1 - d_1)$
DE	$\frac{x_c + p_1 + d_1 + g}{2}$	$Z_c(x_p)$	$\beta_0\ (p_1 + d_1 + g - x_c)$
EF	$p_1 + d_1 + g + \frac{d_2}{2}$	$Z_c(x_p)$	$\beta_0\, d_2\, [\epsilon_w(x_p)]^{\frac{1}{2}}$

C. Quasi-Static Model

In [17] and [18], a quasi-static model was used to derive the transmission-line parameters for the two-port structure consisting of a short length of curved bonding wire in air over a planar dielectric substrate with lower ground plane cladding, like sections BC or EF in Fig. 1(a). As an approximation, such a two-port structure was modeled as a uniform transmission line with characteristic impedance and length equal to that of the original structure. The curved wire was replaced with a straight wire of the same cross section having a constant height above the ground plane. The height of this straight wire is set equal to that of the curved wire in the plane midway between the two-port reference planes. This model and its use in deriving the four-section transmission-line model for the whole structure shown in Fig. 1, as presented below.

1) Single-Wire Interconnection: To apply our quasi-static model to the bonding-wire structure, the interconnection was divided into four intervals corresponding to the sections BC, CD, DE, and EF of Fig. 1(a). Each section was then approximated by a uniform transmission line, as shown in Fig. 3. The electrical lengths and characteristic impedances of these lines were computed by using our quasi-static model to evaluate the local effective dielectric constant $\epsilon_w(x)$ and the local impedance $Z_c(x)$ at the midpoints between B and C, C and D, D and E, and E and F, respectively. These line parameters are given in Table II.

For the single-wire structure, the cross section of the transmission line describing the interconnection consists of a circular wire over a ground plane that may be covered with a dielectric layer, as in sections BC and EF of Fig. 1(a). The quasi-static analysis of such a transmission line is described in [18] and is briefly summarized in the Appendix. From this analysis, the effective dielectric constant and characteristic impedance of the line are given by the following equations:

$$\epsilon_w \approx \left[1 - \frac{k_0}{u_0}\left(\frac{\epsilon_r - 1}{\epsilon_r}\right)\right]^{-(1/2)} \tag{3}$$

$$Z_c = \frac{\eta_0\, u_0}{2\,\pi\,\sqrt{\epsilon_w}} \tag{4}$$

where

$$u_0 = \ln\left(\frac{h}{r_w} + \sqrt{\left(\frac{h}{r_w}\right)^2 - 1}\right) \tag{5}$$

$$k_0 = \ln\left(\frac{\sqrt{\left(\frac{h}{r_w}\right)^2 - 1} + \frac{h_s}{r_w}}{\sqrt{\left(\frac{h}{r_w}\right)^2 - 1} - \frac{h_s}{r_w}}\right). \tag{6}$$

In these expressions, h is the height of the wire from the ground plane, h_s is the thickness of the dielectric substrate, r_w is the radius of the wire, and $\eta_0 = 120\,\pi\,\Omega$ is the wave impedance of a vacuum.

The $\epsilon_w(x_p)$ and $Z_c(x_p)$ values in Table II can then be computed by using (3)–(6) with the values of h, h_s and ϵ_r at the midpoints $x = x_p$.

The soldering regions can be described by a three-conductor transmission line (wire, strip, ground plane). It can be easily seen that, for small electrical lengths, each soldering region AB or FG of Fig. 1(a) can be represented as a T network (see Fig. 3), whose elements are given by[1]

$$C_{s,\,i} = \sqrt{\epsilon_{s,\,i}}\frac{p_i}{c_0}\,\frac{1}{Z_{s,\,i}} \tag{7}$$

$$L_{s,\,i} = \frac{1}{2}\,\sqrt{\epsilon_{s,\,i}}\,\frac{p_i}{c_0}\,Z_{s,\,i} \tag{8}$$

$$C_i = C_{s,\,i} + C_{f,\,i} \tag{9}$$

$$L_{w,\,i} = L_{s,\,i} + \frac{\mu_0}{2\,\pi} p_i \ln\left(\frac{h_{w,\,i}}{r_w} + \sqrt{\left(\frac{h_{w,\,i}}{r_w}\right)^2 - 1}\right) \tag{10}$$

where

$$h_{w,\,i} = \begin{cases} h\,(p_1/2) - h_1, & \text{if } i = 1 \\ h\,(d_b - p_2/2) - h_2, & \text{if } i = 2. \end{cases} \tag{11}$$

In the above formulas, p_i is the length of the ith soldering region, while $Z_{s,\,i}$ and $\epsilon_{s,\,i}$ are the characteristic impedance and the effective dielectric constant of the ith microstrip line. Note that

[1]The three-conductor transmission line is constituted by wire, strip, and ground. To derive the model of the soldering regions, the strip is assumed as common conductor. The input terminals are strip and ground conductors (plane A or G of Fig. 1). The output terminals are wire and ground conductors (plane B or F of Fig. 1). In a first approximation, the coupling between the wire- and ground-strip lines has been neglected. The two-port description of each soldering region is obtained by properly terminating the two lines, i.e., by shorting the wire-strip line at the soldering point and by loading the ground-strip line with the fringing capacitance at the open microstrip end. The T network have been derived by further simplifying this two-port description under the assumption of small electrical lengths. Note that the coupling between the two lines can be neglected only when the wire is close to the strip.

$C_{s,i}/p_i$ and 2 $L_{s,i}/p_i$ are the capacitance and inductance per unit length of the microstrip line.

In (9), $C_{f,i}$ is the fringing capacitance associated with the microstrip open end. Such a capacitance is usually computed with approximate formulas (see [19]) under the assumption of an infinite substrate ($d_d = \infty$, d_d is the distance between the microstrip open-end and the substrate boundary). This leads to considerable errors when $d_d < h_s$. In such cases, a more rigorous model is necessary to account for the substrate truncation. The reactances associated with microstrip open ends on both an infinite ($d_d = \infty$) or finite ($d_d = 75$ μm) substrate have been computed with the FDTD method. The substrate height is $h_s = 254$ μm with $\epsilon_r = 9.86$, the microstrip width is $w = 244$ μm. By fitting the FDTD results, the associated capacitances have been determined. Such capacitance reduces from $C_f = 12.5$ fF for $d_d = \infty$ to $C_f = 7.4$ fF for $d_d = 75$ μm. While the formula in [19] is in good agreement with the former case, an error of about 70% would occur in the latter case.

The lateral offset of the wire with respect to the microstrip has been neglected here since the equivalent series inductance of the interconnection increases only a few percent as the wire moves from the center to the side of the microstrip [11].

2) Double-Wire Interconnection: A quasi-static model of a double-wire structure can be obtained by a proper modification of the above formulas. The cross section of the transmission line describing this interconnection consists of a pair of circular wires over a ground plane that may be covered with a dielectric layer, as in sections BC and EF of Fig. 1(b). The electric potential of the wires is assumed to be the same. Since a conformal mapping analysis of this geometry is difficult to obtain because of the presence of the dielectric substrate, the model has been further simplified assuming an air-filled line, also in sections BC and EF. According to Hilberg [20], the characteristic impedance of this line is given by

$$Z_c = \frac{\eta_0}{4\pi} \ln\left(\frac{2h\sqrt{s^2+4h^2}}{sr_w}\right) \tag{12}$$

where s is the spacing between the two wires. Similarly to the single-wire case, the $Z_c(x_p)$ values in Table II can be computed by using (12) with the value of h at each $x = x_p$. The effective dielectric constant to use in Table II is $\epsilon_w(x) = 1$ because of the above assumption. To complete the model, the inductance defined in (10) must be replaced by

$$L_{w,i} = L_{s,i} + \frac{\mu_0}{4\pi} p_i \ln\left(\frac{2h_{w,i}\sqrt{s^2+4h_{w,i}^2}}{sr_w}\right). \tag{13}$$

III. Validation

The FDTD model was validated first by comparing the simulation results with experimental data available in the literature [17]. Since the FDTD model is shown to provide very accurate results, it has been used as a reference for the quasi-static model. In this way, accuracy and ranges of applicability of the quasi-static model have been assessed by considering several test cases for which measurements were not available.

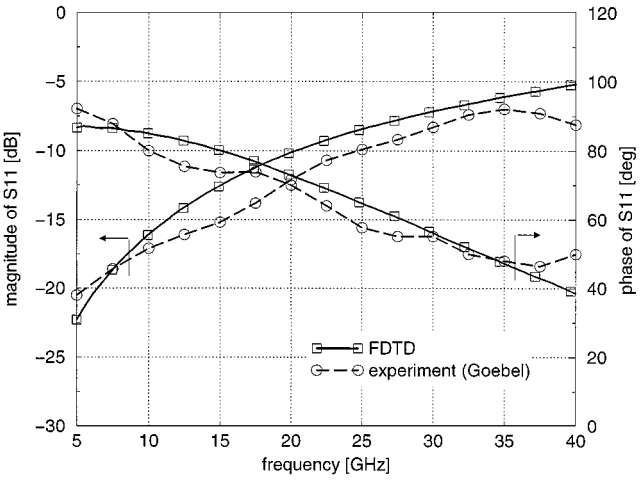

Fig. 4. Comparison between FDTD and experiment. S_{11} of the reference structure. The dimensions of the interconnection are $r_w = 8.5$ μm, $w_1 = w_2 = 244$ μm, $d_b = 470$ μm, $g = 0$ μm, $p_1 = p_2 = 56$ μm, $d_1 = d_2 = 179$ μm, $h_b = 344$ μm, $h_1 = h_2 = 254$ μm, and $\epsilon_{r,1} = \epsilon_{r,2} = 9.86$.

A. Validation of the FDTD Model

To validate the FDTD model, the single-wire interconnect experimented by Goebel [17] has been simulated. Fig. 4 shows the comparison between the computed S_{11} and the measurements. The dimensions of the structure are given in the figure caption; $g = 0$ means that no air gap is present since both microstrips are on the same substrate ($h_1 = h_2$ and $\epsilon_{r,1} = \epsilon_{r,2}$). The main discretization parameters are $\Delta x_{\min} = 5.9$ μm, $\Delta y_{\min} = 17.0$ μm, $\Delta z_{\min} = 10.8$ μm, $\Delta t = 16.5$ fs, and $Bw = 50$ GHz. The agreement of the numerical simulation with the experiment is satisfactory and is within the accuracy of the measurements.

The CPU time for a complete FDTD simulation is about 60 min on a Pentium II 233-MHz platform with Linux operating system. The dimensions of the grid are $N_x \times N_y \times N_z = 35 \times 46 \times 101$ cells and the simulation runs for 50 000 time steps. The other FDTD simulations carried out in this paper have about the same size and require approximately the same computation time.

B. Validation of the Quasi-Static Model

The accuracy of the quasi-static models have been checked against FDTD results using the interconnection between two Al_2O_3 substrates as a test case, for various combinations of lengths and heights of the structure.

1) Single-Wire Interconnection: Two single-wire interconnections have been considered with increasing bonding-wire lengths from 425 to 1300μm. The maximum height of the bonding wire h_b was 354 μm in all cases. Fig. 5 shows the scattering parameter S_{11} of these structures. The agreement of the quasi-static model [see Fig. 3] with the FDTD simulation is excellent. In the quasi-static model, the value of the fringing capacitances is $C_f = 7.4$ fF.

In order to analyze the effect of the wire curvature, two additional structures have been analyzed with wire height ranging from 454 to 524 μm, while the length d_b in each case is 550 μm.

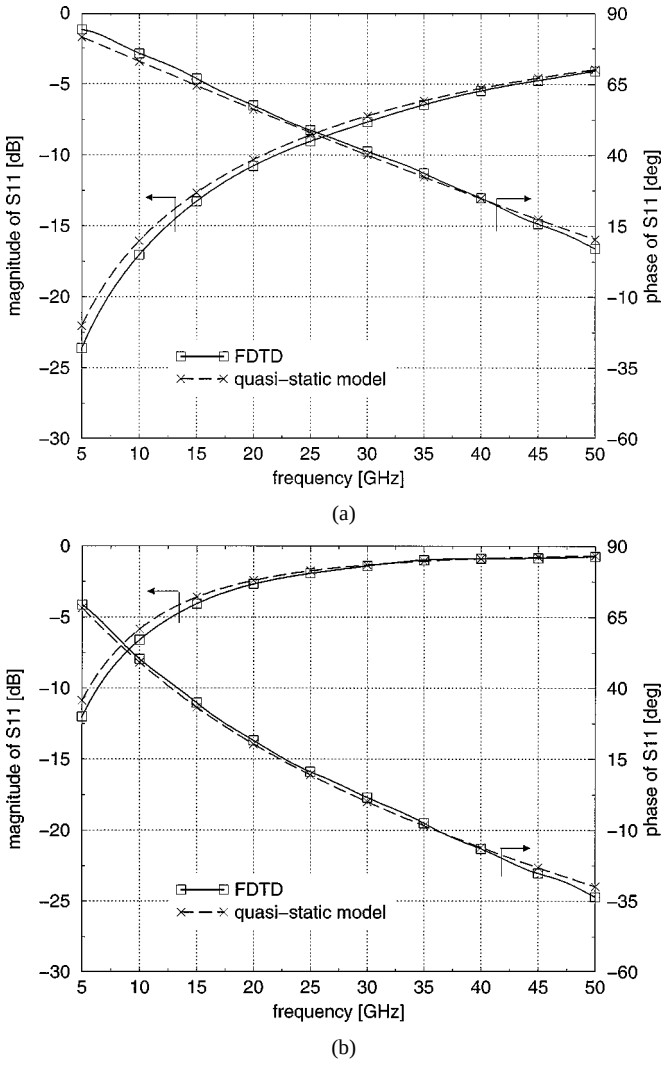

Fig. 5. Comparison between FDTD and quasi-static model in the case of a single-wire interconnection. S_{11} is plotted for two bonding-wire lengths. (a) $d_b = 425\ \mu$m. (b) $d_b = 1300\ \mu$m. The dimensions of the structure are $r_w = 8.5\ \mu$m, $w_1 = w_2 = 244\ \mu$m, $h_b = 354\ \mu$m, $p_1 = p_2 = 75\ \mu$m, $d_1 = d_2 = 75\ \mu$m, $h_1 = h_2 = 254\ \mu$m, and $\epsilon_{r,1} = \epsilon_{r,2} = 9.86$.

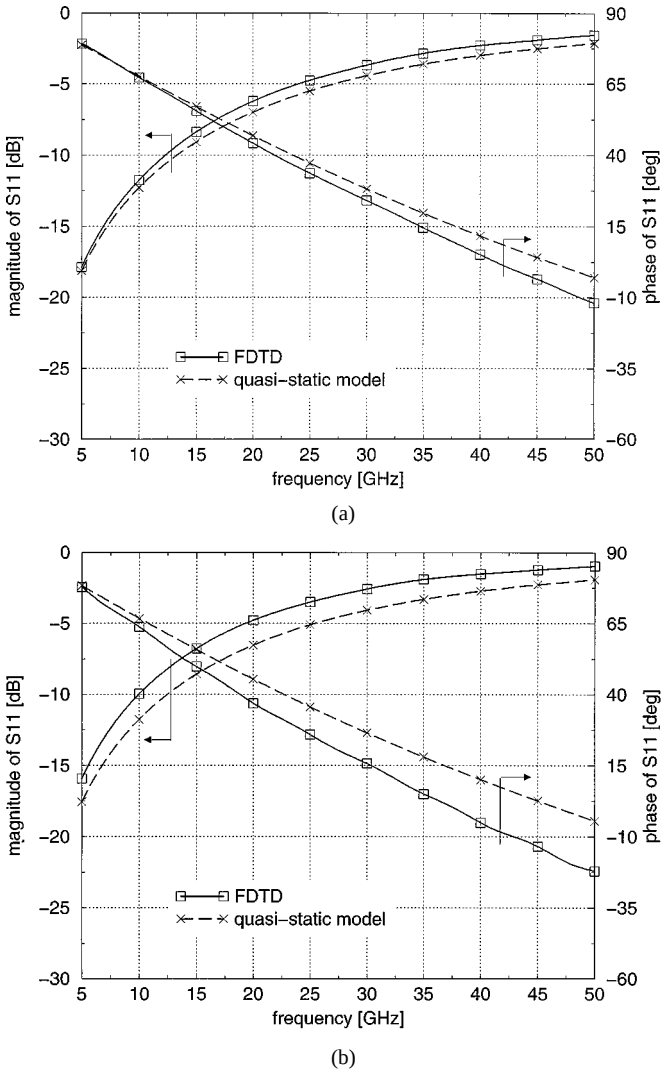

Fig. 6. Comparison between FDTD and quasi-static model in the case of a single-wire interconnection. S_{11} is plotted for two bonding-wire heights. (a) $h_b = 454\ \mu$m. (b) $h_b = 524\ \mu$m. The dimensions of the structure are $r_w = 8.5\ \mu$m, $w_1 = w_2 = 244\ \mu$m, $d_b = 550\ \mu$m, $g = 250\ \mu$m, $p_1 = p_2 = 75\ \mu$m, $d_1 = d_2 = 75\ \mu$m, $h_1 = h_2 = 254\ \mu$m, and $\epsilon_{r,1} = \epsilon_{r,2} = 9.86$.

Note that for $h_b = 524\ \mu$m, the shape of the bonding wire is approximately one-half of a circumference. Fig. 6 shows the computed S_{11}. From the results shown in this figure, it appears that the accuracy of the quasi-static model is acceptable only when the height of the wire is less than about 450 μm (first case). As the height increases, in fact, the model of the soldering regions AB and FG of Fig. 1(a) looses its accuracy. A parameter that can be used to check whether the quasi-static model produces reliable results is the height of the wire with respect to the substrates at positions B and F of Fig. 1(a). When the following condition is satisfied:

$$\max\left[\frac{h(p_1)-h_1}{w_1}, \frac{h(d_b-p_2)-h_2}{w_2}\right] \le \frac{1}{2} \qquad (14)$$

the accuracy of the quasi-static model is better than 1 dB in the magnitude and 10° in the phase of S_{11} [see Fig. 6, case for $h_b = 454\ \mu$m].

The quasi-static model has also been validated in the case multichip interconnections. In particular, an interconnection between a 100-μm-thick GaAs chip and a 254-μm-thick Al_2O_3 substrate has been considered. The FDTD discretization of the simulated structure is shown in Fig. 2. Again, the quasi-static model agrees very well with the FDTD analysis.

2) Double-Wire Interconnection: To validate the quasi-static model for double-wire interconnections, two structures have been considered with wire spacing of $s = 0.23w$ and $s = 0.93w$, where w is the microstrip width. The length and height are $d_b = 470\ \mu$m and $h_b = 344\ \mu$m, respectively, for both cases. The magnitude of S_{11} is shown in Fig. 7. The agreement between the quasi-static model and FDTD simulation is considered to be satisfactory. In the quasi-static model, the fringing capacitances is $C_f = 7.0$ fF.

IV. Characterization

Having checked its accuracy, the quasi-static model has been used for an extensive characterization of the electrical behavior of the bonding wire versus the main geometrical parameters (length, height, and for double-wire, wire spacing). For this pur-

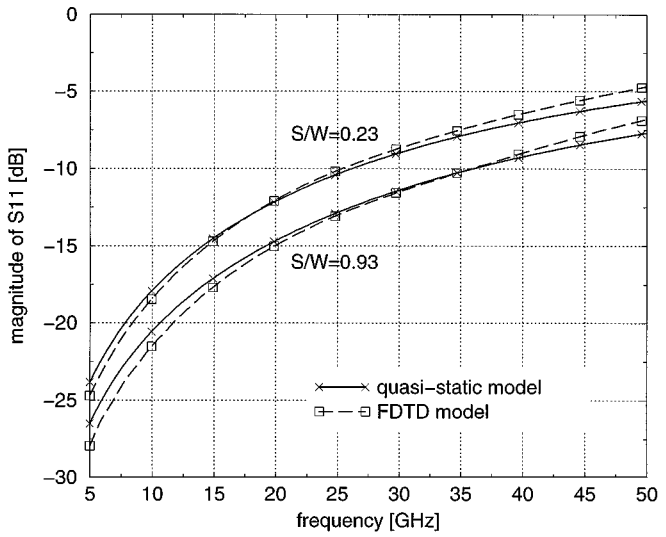

Fig. 7. Comparison between FDTD and quasi-static model in the case of a double-wire interconnection. S_{11} is plotted for two wire spacings. The dimensions of the structure are $r_w = 8.5\ \mu$m, $w_1 = w_2 = 244\ \mu$m, $d_b = 470\ \mu$m, $g = 224\ \mu$m, $p_1 = p_2 = 56\ \mu$m, $d_1 = d_2 = 67\ \mu$m, $h_b = 344\ \mu$m, $h_1 = h_2 = 254\ \mu$m, and $\epsilon_{r,1} = \epsilon_{r,2} = 9.86$.

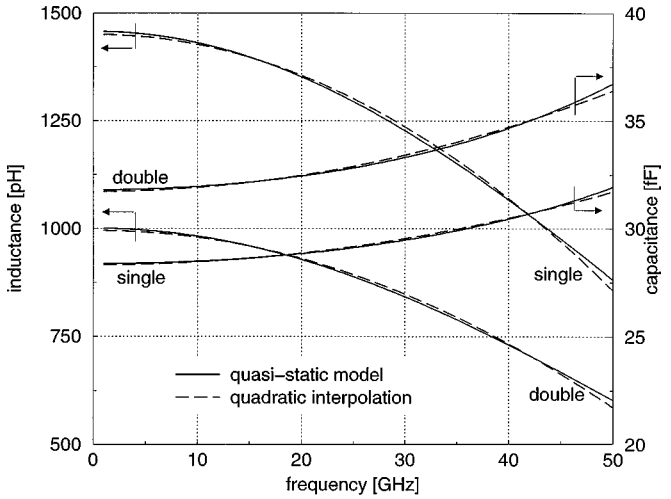

Fig. 8. Equivalent π-parameters versus the frequency. The length of the interconnection is $d_b = 1500\ \mu$m. For the double-wire structure, the wire spacing is $s = 200\ \mu$m. The other dimensions of the structure are: $r_w = 8.5\ \mu$m, $w_1 = w_2 = 244\ \mu$m, $p_1 = p_2 = 75\ \mu$m, $d_1 = d_2 = 75\ \mu$m, $g = 1200\ \mu$m, $h_b = 650\ \mu$m, $h_1 = h_2 = 254\ \mu$m, and $\epsilon_{r,1} = \epsilon_{r,2} = 9.86$.

pose, the quasi-static results (y-matrix) have been converted into a lumped-element π network consisting of a series inductance L and two shunt capacitances C_1 and C_2. These quantities can be calculated as

$$L = \frac{1}{j\omega y_{21}} \tag{15}$$

$$C_1 = \frac{y_{11} + y_{21}}{j\omega} \tag{16}$$

$$C_2 = \frac{y_{22} + y_{21}}{j\omega} \tag{17}$$

where y_{ij} are the elements of the admittance matrix of the quasi-static model. For symmetrical structures ($y_{11} = y_{22}$), $C_1 = C_2$. As an example, the equivalent π-parameters are shown in Fig. 8 (solid lines) for both single- and double-wire interconnections. The inductance reduction of the double-wire structure with respect to the single-wire configuration is apparent. It is also observed that, in both cases, the inductances decrease of about 40% when the frequency increases from 0 to 50 GHz. At the latter frequency, the wire length is approximately a quarter-wavelength.

The frequency dependence of the equivalent π-parameters can be interpolated with a quadratic law as follows:

$$L = L_0 + L_2\ f^2 \tag{18}$$

$$C_1 = C_{10} + C_{12}\ f^2 \tag{19}$$

$$C_2 = C_{20} + C_{22}\ f^2. \tag{20}$$

In this way, the electrical behavior of the bonding wire can be described by only six (four if the structure is symmetric) parameters. The interpolation coefficients have been evaluated using the least-squares method [21, pp. 650–660]. The results are shown again in Fig. 8 (dashed lines). The interpolation error is within $\pm 1.8\%$ for the inductance and within $\pm 0.6\%$ for the capacitance. These values represent the maximum interpolation errors for $f \leq 50$ GHz and $d_b \leq 1500\ \mu$m.

The interpolation coefficients in (18)–(20) have finally been computed for the representative case of single- and double-wire interconnections between two identical Al_2O_3 substrates. Figs. 9 and 10 show the inductance and capacitance coefficients versus the wire length and for different heights. The other geometrical parameters are $r_w = 8.5\ \mu$m, $w_1 = w_2 = 244\ \mu$m, $p_1 = p_2 = 75\ \mu$m, and $d_1 = d_2 = 75\ \mu$m.

The results presented in those figures can be easily used to predict the electrical behavior of single- and double-wire interconnections in a wide range of parameter variations up to 50 GHz. In particular, to minimize the discontinuity effects, a low-pass filter can be designed embedding the lumped-element equivalent π-network of the bonding wire.

V. Conclusions

Both a FDTD and a quasi-static models of the bonding-wire interconnection have been described in this paper. The quasi-static model allows the analysis of single- and double-wire configurations and is suitable to be implemented in commercial microwave CAD tools. In order to assess the accuracy and applicability of the quasi-static model, several test structures have been analyzed. The reference results have been obtained using the FDTD method. From this systematic study, it emerges that the quasi-static method is very accurate for flat interconnections. Finally, the quasi-static model has been used to provide an extensive electrical characterization of the bonding wire versus its main geometrical parameters. The characterization is given in terms of an equivalent low-pass π-network, which is composed by a series inductance and two shunt capacitances. This representation can be easily exploited in the design of matching networks capable of increasing the bandwidth of the interconnection.

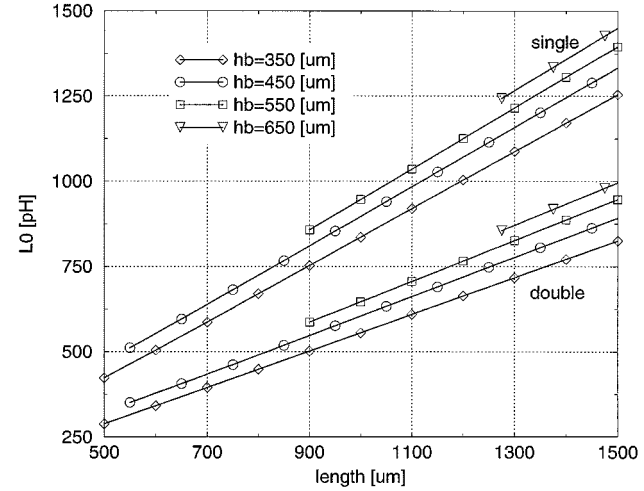

(a)

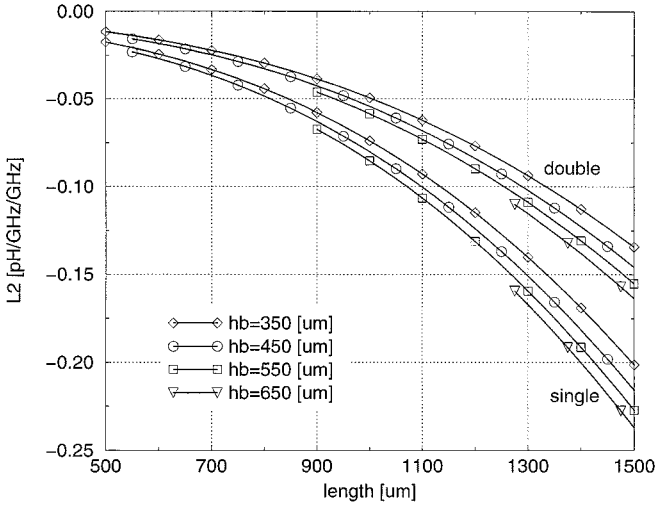

(b)

Fig. 9. Coefficients of the equivalent series inductance versus d_b. For the double-wire interconnection, $s = 200$ μm. (a) Zeroth-order inductance. (b) Second-order coefficient.

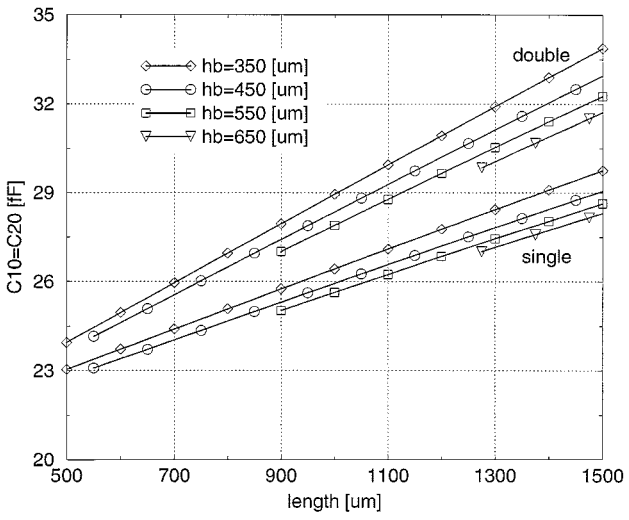

(a)

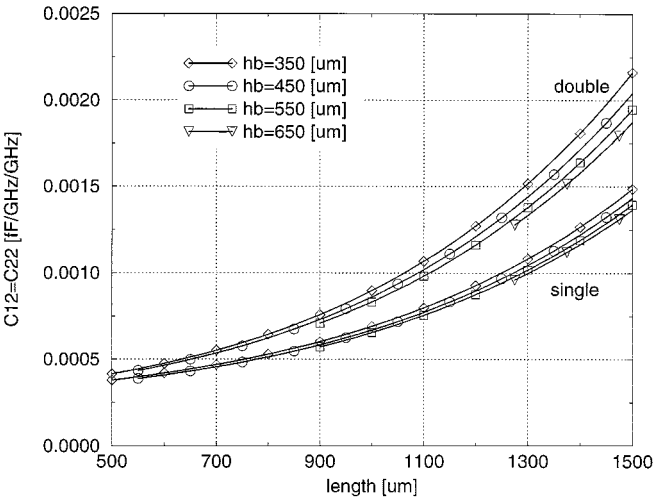

(b)

Fig. 10. Coefficients of the equivalent shunt capacitance versus d_b. For the double-wire interconnection, $s = 200$ μm. (a) Zeroth-order capacitance. (b) Second-order coefficient.

APPENDIX

The quasi-static analysis of a straight wire line at a constant height over a ground plane covered with a dielectric layer was carried out in [18]. In this paper, the effective dielectric constant of such a transmission line will be derived using an approximation. To do this, we use the conformal mapping method described in [18] to transform the cross-sectional geometry of the wire line into a parallel-plate capacitor partially filled with dielectric material. The u coordinate of the curved dielectric surface in this u, v coordinate system can be approximated by the following function of v:

$$f(v) \approx \frac{k_0}{2}(1 - \cos v) \tag{21}$$

where k_0 is the maximum thickness (or u coordinate) of the dielectric region. The value of k_0 is evaluated by substituting h_s for z in the following complex mapping function:

$$e^{u+jv} = \frac{z + \sqrt{h^2 - r_w^2}}{z - \sqrt{h^2 - r_w^2}} \tag{22}$$

and then solving for u, since $k_0 = u$ when $z = h_s$. The result is given in (6). The line capacitance C can be evaluated from $f(v)$ by using the following integral:

$$C \approx 2\frac{\epsilon_0}{u_0}\int_{-\pi}^{0} \frac{dv}{1 - \dfrac{1}{u_0}\left(\dfrac{\epsilon_r - 1}{\epsilon_r}\right) f(v)} \tag{23}$$

as explained in [18]. Here, u_0 is the distance between the plates of the transformed capacitor, and is given by (5), also explained in [18]. The effective dielectric constant of the line is then derived by the following:

$$\epsilon_w = \frac{C}{C_0} \tag{24}$$

where C_0 is the capacitance per unit length of the air-filled structure. As shown in [18], this is given by

$$C_0 = \frac{2\pi\epsilon_0}{u_0}. \tag{25}$$

Equation (3) is obtained by simply inserting (21) in (23) and using (25). The range of validity of (3) has been determined by computing the effective dielectric constant with the finite-difference (FD) method [22, pp. 166–172]. The cross section of the wire line is modeled as being enclosed in a metallic box. The size of the box was chosen so as not to alter the field distribution significantly. The comparison between the approximate formula (3) and FD shows that the error increases for small $t/r_w = h/r_w - h_s/r_w - 1$ and high h_s/r_w. The accuracy of (3) is better than 5% for $t/r_w > 4$, $h_s/r_w < 20$, and $\epsilon_r < 10$. For $t/r_w \gg 1$, (3) agrees well with the formula published in [23, p. 1067].

ACKNOWLEDGMENT

The authors would like to thank U. Goebel, Daimler Benz Aerospace, Ulm, Germany, and the reviewers for their helpful suggestions and comments.

REFERENCES

[1] M. Boheim and U. Goebel, "Low-cost packages for micro- and millimeter-wave circuits," in *24th European Microwave Conf.*, Cannes, France, Sept. 1994, pp. 122–132.

[2] H. Jin, R. Vahldieck, J. Huang, and P. Russer, "Rigorous analysis of mixed transmission line interconnects using the frequency-domain TLM method," *IEEE Trans. Microwave Theory Tech.*, vol. 41, pp. 2248–2255, Nov. 1993.

[3] H. Lee, "Wide-band characterization of a typical bonding wire for microwave and millimeter-wave integrated circuits," *IEEE Trans. Microwave Theory Tech.*, vol. 43, pp. 63–68, Jan. 1993.

[4] S. K. Yun and H. Y. Lee, "Parasitic impedance analysis of double bonding wire for high frequency integrated circuits packaging," *IEEE Microwave Guided Wave Lett.*, vol. 5, pp. 296–298, Sept. 1995.

[5] R. Vahldieck, S. Chen, H. Jin, and P. Russer, "Flip-chip and bond wire/airbridge transitions between passive microwave transmission lines and laser diodes," in *25th European Microwave Conf.*, Bologna, Italy, Sept. 1995, pp. 875–878.

[6] G. Baumann, D. Ferling, and H. Richter, "Comparison of flip chip and wire bond interconnections and the technology evaluation on 51 GHz transceiver modules," in *26th European Microwave Conf.*, vol. 1, Prague, Czech Republic, Sept. 1996, pp. 98–100.

[7] T. Krems, W. Haydl, H. Massler, and J. Rudiger, "Millimeter-wave performance of chip interconnections using wire bonding and flip chip," in *IEEE MTT-S Int. Microwave Symp. Dig.*, vol. 1, San Francisco, CA, June 1996, pp. 247–250.

[8] G. Strauss and W. Menzel, "A novel concept for MM-wave MMIC interconnects and packaging," in *IEEE MTT-S Int. Microwave Symp. Dig.*, San Diego, CA, May 1994, pp. 1141–1144.

[9] F. Alimenti, W. Menzel, P. Mezzanotte, L. Roselli, and R. Sorrentino, "Analisi FDTD di connessioni ad accoppiamento elettromagnetico per circuiti integrati monolitici a onde millimetriche," in *XI Riunione Naz. Elettromag.*, Firenze, Italy, Oct. 1996, pp. 37–40.

[10] F. Alimenti, P. Mezzanotte, and L. Roselli, "Full-wave investigation on the curved bonding wire interconnection by using a suitable FDTD code," in *IEEE MTT-S Int. Microwave Symp. Dig.*, Denver, CO, June 1997, pp. 1737–1740.

[11] F. Alimenti, P. Mezzanotte, L. Roselli, and R. Sorrentino, "Multi-wire microstrip interconnections: A systematic analysis for the extraction of an equivalent circuit," in *IEEE MTT-S Int. Microwave Symp. Dig.*, vol. 3, Baltimore, MD, June 1998, pp. 1929–1932.

[12] D. H. Choi and V. Hoefer, "A graded mesh FD-TD algorithm for eigenvalue problems," in *17th European Microwave Conf.*, Roma, Italy, Sept. 1987, pp. 413–417.

[13] P. Mezzanotte, L. Roselli, and R. Sorrentino, "A simple way to model curved surfaces in FDTD algorithm avoiding staircase approximation," *IEEE Microwave Guided Wave Lett.*, vol. 5, pp. 267–269, Aug. 1995.

[14] W. Heinrich, K. Beilenhoff, P. Mezzanotte, and L. Roselli, "On the accuracy of the finite difference method using mesh grading," *IEEE Trans. Microwave Theory Tech.*, vol. 44, pp. 1569–1574, Sept. 1996.

[15] S. D. Gedney, "An anistropic perfectly matched layer-absorbing medium for the truncation of FDTD lattices," *IEEE Trans. Microwave Theory Tech.*, vol. 44, pp. 1630–1639, Dec. 1996.

[16] A. P. Zhao and A. V. Raisanen, "Application of a simple and efficient source excitation technique to the FDTD analysis of waveguide and microstrip circuits," *IEEE Trans. Microwave Theory Tech.*, vol. 44, pp. 1535–1539, Sept. 1996.

[17] U. Goebel, "DC to 100 GHz chip-to-chip interconnects with reduced tolerance sensitivity by adaptive wirebonding," in *3rd Topical Elect. Performance Electron. Packag. Meeting*, Monterey, CA, Nov. 1994, pp. 182–185.

[18] F. Alimenti, U. Goebel, and R. Sorrentino, "Quasi-static analysis of microstrip bondwire interconnects," in *IEEE MTT-S Int. Microwave Symp. Dig.*, vol. 2, Orlando, FL, May 1995, pp. 679–682.

[19] N. G. Alexopoulos and S.-C. Wu, "Frequency-independent equivalent circuit model for microstrip open-end and gap discontinuities," *IEEE Trans. Microwave Theory Tech.*, vol. 42, pp. 1268–1272, July 1994.

[20] W. Hilberg, *Electrical Characteristics of Transmission Lines*. Norwood, MA: Artech House, 1979.

[21] W. H. Press, S. A. Teukolsky, W. T. Vetterling, and B. P. Flannery, *Numerical Recipes*. Cambridge, U.K.: Cambridge Univ. Press, 1992.

[22] M. Sadiku, *Numerical Techniques in Electromagnetics*. Boca Raton, FL: CRC Press, 1992.

[23] E. F. Kuester and D. C. Chang, "Propagating modes along a thin wire located above a grounded dielectric slab," *IEEE Trans. Microwave Theory Tech.*, vol. 25, pp. 1065–1069, Dec. 1977.

Federico Alimenti (S'91–A'93) was born in Foligno, Italy, in 1968. He received the Laurea (*cum laude*) and the Ph.D. degrees from the University of Perugia, Perugia, Italy, in 1993 and 1997, respectively, both in electronic engineering.

In 1993, he was with the Microwave and Millimeter-Wave Department, Daimler Benz Aerospace, Ulm, Germany. In 1996, he was a Guest Scientist at the Lehrstuhl fur Hochfrequenztechnik, Technical University of Munchen, Munich, Germany. In 1997, he visited the Technical University of Munchen, under the Vigoni Program. Since 1993, he has been with the Department of Electronic and Information Engineering, University of Perugia. His research interests concern the FDTD simulation of microwave and millimeter-wave devices, the study of MMIC interconnection and packaging technologies, and the design, realization, and measurement of high-frequency circuits.

Dr. Alimenti has been a reviewer for the IEEE MICROWAVE AND GUIDED WAVE LETTERS since 1997. He was the recipient of a 1993 Daimler Benz Aerospace Scholarship and was awarded the 1996 Young Scientist Award presented by the URSI.

Paolo Mezzanotte was born in Perugia, Italy, in 1965. He received the Laurea degree in electronic engineering from the University of Ancona, Ancona, Italy, in 1991 (his thesis concerned FDTD analysis of the GTEM cell), and the Ph.D. degree from the University of Perugia, Perugia, Italy, in 1997.

Since 1992, he has been involved with FDTD analysis of microwave structures in cooperation with the Department of Electronic and Information Engineering, University of Perugia. His main field of interest is the application of numerical methods to the study of components and structures for microwave and millimeter-wave circuits.

Luca Roselli (M'93) was born in Florence, Italy, in 1962. He received the Laurea degree in electronic engineering from the University of Florence, Florence, Italy, in 1988.

From 1988 to 1991, he was with the University of Florence, where he was involved with surface acoustic wave (SAW) devices. In November 1991, he joined the Department of Electronic and Information Engineering, University of Perugia, Perugia, Italy, as a Research Assistant, where, since 1994, he has taught the "Electronic Devices" course. His research interests include the design and development of microwave and millimeter-wave active and passive circuits by numerical techniques.

Dr. Roselli has been on the Technical Committee of the Electrosoft Conference, European Microwave Conference, and IEEE Microwave Theory and Techniques Symposium since 1996. He has been a reviewer for the IEEE MICROWAVE AND GUIDED WAVE LETTERS (since 1996) and the IEEE TRANSACTIONS ON MICROWAVE THEORY AND TECHNIQUES (since 1998).

Roberto Sorrentino (M'77–SM'84–F'90) received the Doctor degree in electronic engineering from the University of Rome "La Sapienza," Rome, Italy, in 1971.

In 1971, he joined the Department of Electronics, University of Rome "La Sapienza," where he became an Assistant Professor in 1974. He was also Professore Incaricato at the University of Catania (1975–76), the University of Ancona (1976–77), and the University of Rome "La Sapienza" (1977–1982), where he was then an Associate Professor (1982–1986). In 1983 and 1986, he was a Research Fellow at The University of Texas at Austin. From 1986 to 1990, he was a Professor at the Second University of Rome "Tor Vergata." Since November 1990, he has been a Professor at the University of Perugia, Perugia, Italy, where he was the Chairman of the Electronic Institute and Director of the Computing Center, and is currently the Dean of the Faculty of Engineering. His research activities have been concerned with electromagnetic-wave propagation in anisotropic media, interaction with biological tissues and, mainly, with the analysis and design of microwave and millimeter-wave passive circuits. He has contributed to the planar-circuit approach for the analysis of microstrip circuits and to the development of numerical techniques for the modeling of components in planar and quasi-planar configurations. He in an Editorial Board member for the *International Journal of Numerical Modeling* and the *International Journal of Microwave and Millimeter-Wave Computer-Aided Engineering*.

Dr. Sorrentino is currently an Editorial Board member for the IEEE TRANSACTIONS ON MICROWAVE THEORY AND TECHNIQUES.